

Which One Is Preferred: Myers–Saito Cyclization of Ene-Yne-Allene or Garratt–Braverman Cyclization of Conjugated Bisallenic Sulfone? A Theoretical and Experimental Study

Amit Basak,^{*,†} Sanket Das,[†] Dibyendu Mallick,[‡] and Eluvathingal D. Jemmis^{*,‡,§}

Department of Chemistry, Indian Institute of Technology, Kharagpur 721 302, India, Department of Inorganic and Physical Chemistry, Indian Institute of Science, Bangalore 560 012, India, and Indian Institute of Science Education and Research Thiruvananthapuram, CET Campus, Thiruvananthapuram, 695 016 Kerala, India

Received April 3, 2009; E-mail: absk@chem.iitkgp.ernet.in

Abstract: A competitive scenario between Myers–Saito (MS) and Garratt–Braverman (GB) cyclization has been created in a molecule. High-level computations indicate a preference for GB over MS cyclization. The activation energies for the rate-determining steps of the GB and MS cyclizations were found to be the same (24.4 kcal/mol) at the B3LYP/6-31G* level of theory; thus, from the kinetic point of view, both reactions are feasible. However, the main biradical intermediate **GB2** of the GB reaction is 6.2 kcal/mol lower in energy than the biradical **MS2**, which is the main intermediate of MS reaction, so GB cyclization is thermodynamically favored over MS cyclization. To verify the prediction by computational techniques, bisenediynyl sulfones **1–4** and bisenediynyl sulfoxide **17** were synthesized. Under basic conditions, these molecules isomerized to a system possessing both the ene-yne-allene and the bisallenic sulfone. The isolation of only one product, identified as the corresponding naphthalene- or benzene-fused sulfone **8–11**, indicated the occurrence of GB cyclization as the sole reaction pathway. No product corresponding to the MS cyclization pathway could be isolated. Though the theoretical prediction showed a preference for the GB pathway over the MS pathway, the exclusive preference for GB over MS cyclization is very striking. Further analysis showed that the intramolecular self-quenching nature of the GB pathway may play an important role in the complete preference for this reaction. Apart from the mechanistic studies, these sulfones showed DNA cleavage activity that had an inverse relation with the reactivity order. Our findings are important for the design of artificial DNA-cleaving agents.

Ever since the discovery of enediyne antibiotics in the 1980s,¹ the chemistry of spontaneous generation of diradicals has attracted quite unprecedented attention² because of their role in organic synthesis,³ in the preparation of new materials,⁴ and

especially in pharmacology.¹ Acting as natural antibiotics, these molecules destroy the DNA of bacteria and viruses, and their cytotoxic activity has been exploited in the development of anticancer agents.⁵ The DNA-damaging activities of these molecules depend upon their ability to abstract hydrogen atoms from various locations of the deoxyribose moiety (Scheme 1). However, not all diradicals are generated spontaneously under ambient conditions. Also, not all of them have the same efficiency of H abstraction. It is those diradicals that do not have any mechanism of self-quenching that become diamagnetic via abstraction of atoms from external sources. Bergman cyclization (BC)⁶ and related reactions such as Myers–Saito (MS) cyclization⁷ belong to this category. On the other hand, reactions such as Garratt–Braverman (GB) cyclization⁸ involving conjugated bisallenes (Scheme 2) have a self-quenching mechanism, and hence, the chances of interaction with external

[†] Indian Institute of Technology Kharagpur.

[‡] Indian Institute of Science.

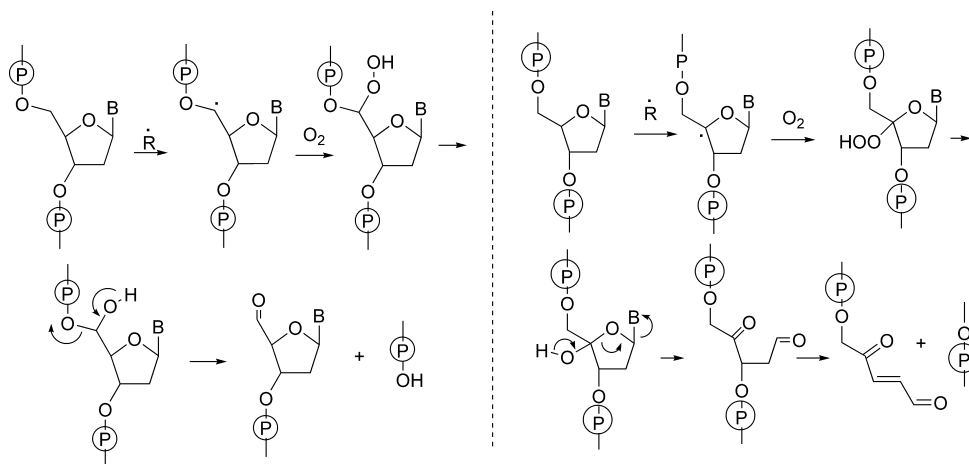
[§] Indian Institute of Science Education and Research Thiruvananthapuram.

- (1) (a) *Enediyne Antibiotics as Antitumor Agents*; Border, D. B., Doyle, T. W., Eds.; Marcel Dekker: New York, 1995. (b) *Cancer Chemotherapeutic Agents*; Foye, W. O., Ed.; American Chemical Society: Washington, DC, 1995.
- (2) (a) Basak, A.; Mandal, S.; Bag, S. S. *Chem. Rev.* **2003**, *103*, 4077. (b) Krohn, K. *Angew. Chem., Int. Ed.* **2006**, *45*, 536. (c) Saito, I.; Nakatani, K. *Bull. Chem. Soc. Jpn.* **1996**, *69*, 3007. (d) Wenk, H. H.; Winkler, M.; Sander, W. *Angew. Chem., Int. Ed.* **2003**, *42*, 502. (e) Maier, M. E.; Bosse, F.; Niestroj, A. *J. Eur. J. Org. Chem.* **1999**, 1. (f) Nicolaou, K. C.; Smith, A. L. *Modern Acetylene Chemistry*; Stang, P. J., Diederich, F., Eds.; VCH: Weinheim, Germany, 1995; pp 203–283; (g) Maier, M. E. *Synlett* **1995**, 13. (h) *DNA and RNA Cleavers and Chemotherapy of Cancer and Viral Diseases*; Meunier, B., Ed.; Kluwer: Dordrecht, The Netherlands, 1996; p 372.
- (3) (a) Grissom, J. W.; Gunawardena, G. U.; Klinberg, D.; Huang, D. *Tetrahedron* **1996**, *52*, 6453. (b) Schreiner, P. R.; Prall, M.; Lutz, V. *Angew. Chem., Int. Ed.* **2003**, *42*, 5757.
- (4) (a) Perpall, M. W.; Perera, K. P. U.; DiMaio, J.; Ballato, J.; Foulger, S. H.; Smith, D. W., Jr. *Langmuir* **2003**, *19*, 7153. (b) John, J. A.; Tour, J. M. *Tetrahedron* **1997**, *53*, 15515.

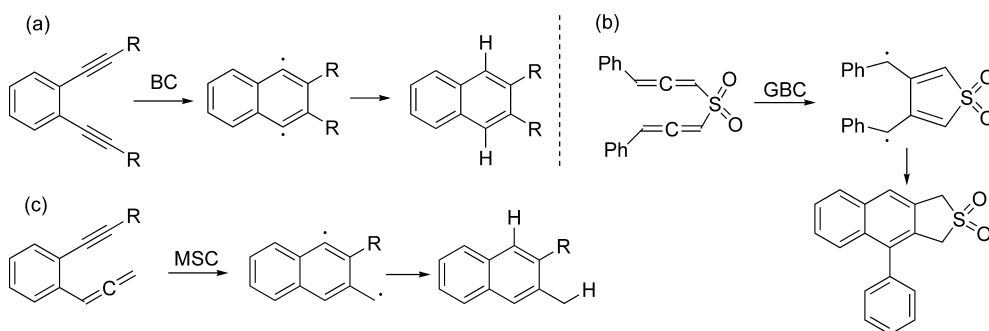
(5) Bross, P. F.; Beitz, J.; Chen, G.; Chen, X. H.; Duffy, E.; Kieffer, L.; Roy, S.; Sridhara, R.; Rahman, A.; Williams, G.; Pazdur, R. *Clin. Cancer Res.* **2001**, *7*, 1490.

(6) (a) Jones, R. G.; Bergman, R. G. *J. Am. Chem. Soc.* **1972**, *94*, 660. (b) Bergman, R. G. *Acc. Chem. Res.* **1973**, *6*, 25. (c) Lockhart, T. P.; Bergman, R. G. *J. Am. Chem. Soc.* **1981**, *103*, 4091. (d) Nicolaou, K. C.; Zuccarello, G.; Oogawa, Y.; Schweiger, E. J.; Kumazawa, T. *J. Am. Chem. Soc.* **1988**, *110*, 4866. (e) Gaffney, S. H.; Capitani, J. F.; Castado, L.; Mitra, A. *Int. J. Quantum Chem.* **2003**, *95*, 706.

Scheme 1. Mechanisms of Phosphodiester Bond Cleavage Induced by Radicals: Damage via 5'-H and 4'-H Abstraction Are Shown, and Other Abstraction Processes Are Also Possible



Scheme 2. Generation of a Biradical through (a) Bergman Cyclization (BC), (b) Garratt–Braverman Cyclization (GBC), and (c) Myers–Saito Cyclization (MSC)



sources are slim. BC is usually a slow process with a high activation energy unless the enediyne is constrained in a ring system of the proper size, as in the natural product calicheamicin.⁹ On the other hand, MS cyclization involving ene-yne-allenes⁷ takes place spontaneously under ambient conditions, even for acyclic systems. The latter chemistry is shown by the neocarzinostatin (NCS) chromophore¹⁰ when it acts as an antitumor agent. Nicolaou et al.¹¹ first attempted to utilize GB cyclization chemistry in bisallenic sulfones. However, the DNA

cleavage exhibited by these molecules mostly involved Michael addition of a DNA base followed by Maxam–Gilbert-type¹² cleavage rather than proceeding via H abstraction. Nonetheless, this observation provided an alternative way of inducing DNA cleavage. GB rearrangement generally takes place at higher temperature unless the allenes are further conjugated, in which case the reaction takes place under ambient conditions.¹³ The biological relevance of all these reactions, along with their challenging electronic structures, demanded the attention of computational chemists to apply theoretical methodologies to these systems and, if possible, take a leading role in predicting the outcome in case of substrates endowed with various possible pathways. Though many theoretical studies have been devoted to BC processes,¹⁴ computational studies of MS cyclization are

- (7) (a) Nagata, R.; Yamanaka, H.; Okazaki, E.; Saito, I. *Tetrahedron Lett.* **1989**, *30*, 4995. (b) Myers, A. G.; Kuo, E. Y.; Finney, N. S. *J. Am. Chem. Soc.* **1989**, *111*, 8057. (c) Myers, A. G.; Dragovich, P. S. *J. Am. Chem. Soc.* **1989**, *111*, 9130. (d) Nagata, R.; Yamanaka, H.; Murahashi, E.; Saito, I. *Tetrahedron Lett.* **1990**, *31*, 2907.
- (8) (a) Braverman, S.; Segev, D. *J. Am. Chem. Soc.* **1974**, *96*, 1245. (b) Garratt, P. J.; Neoh, S. B. *J. Org. Chem.* **1979**, *44*, 2667. (c) Cheng, Y. S. P.; Garratt, P. J.; Neoh, S. B.; Rumjanek, V. H. *Isr. J. Chem.* **1985**, *26*, 101. (d) Braverman, S.; Duar, Y.; Segev, D. *Tetrahedron Lett.* **1976**, *17*, 3181. (e) Zafrani, Y.; Gottlieb, H. E.; Sprecher, M.; Braverman, S. *J. Org. Chem.* **2005**, *70*, 10166.
- (9) (a) Lee, M. D.; Dunne, T. S.; Chang, C. C.; Ellestad, G. A.; Siegel, M. M.; Morton, G. O.; McGahren, W. J.; Borders, D. B. *J. Am. Chem. Soc.* **1987**, *109*, 3466. (b) Zein, N.; Sinha, A. M.; McGahren, W. J.; Ellestad, G. A. *Science* **1988**, *240*, 1198. (c) Zein, N.; Poncin, M.; Nilakantan, R.; Ellestad, G. A. *Science* **1989**, *244*, 697. (d) Ellestad, G. A.; Hammann, P. R.; Zein, N.; Morton, G. O.; Siegel, M. M.; Patel, M.; Borders, D. B.; McGahren, W. J. *Tetrahedron Lett.* **1989**, *30*, 3033. (e) Magnus, P.; Carter, P. J. *J. Am. Chem. Soc.* **1989**, *111*, 7630. (f) Mantlo, N. B.; Danishefsky, S. *J. Org. Chem.* **1989**, *54*, 2781. (g) Chatterjee, M.; Cramer, K. D.; Townsend, C. A. *J. Am. Chem. Soc.* **1993**, *115*, 3374.
- (10) (a) Myers, A. G. *Tetrahedron Lett.* **1987**, *28*, 4493. (b) Myers, A. G.; Proteau, P. J. *J. Am. Chem. Soc.* **1988**, *110*, 1146.
- (11) Nicolaou, K. C.; Wendeborn, S.; Maligres, P.; Isshiki, K.; Zein, N.; Ellestad, G. *Angew. Chem., Int. Ed. Engl.* **1991**, *30*, 418.

- (12) (a) Maxam, A. M.; Gilbert, W. *Methods Enzymol.* **1980**, *65*, 499. (b) Maxam, A. M.; Gilbert, W. *Proc. Natl. Acad. Sci. U.S.A.* **1977**, *74*, 560.
- (13) Braverman, S.; Zafrani, Y.; Gottlieb, H. E. *Tetrahedron Lett.* **2000**, *41*, 2675.
- (14) (a) Lindh, R.; Persson, B. J. *J. Am. Chem. Soc.* **1994**, *116*, 4963. (b) Lindh, R.; Lee, T. J.; Bernhardtsson, A.; Persson, B. J.; Karlström, G. *J. Am. Chem. Soc.* **1995**, *117*, 7186. (c) Kraka, E.; Cremer, D.; Bucher, G.; Wandel, H.; Sander, W. *Chem. Phys. Lett.* **1997**, *268*, 313. (d) Kraka, E.; Cremer, D. *J. Am. Chem. Soc.* **1994**, *116*, 4929. (e) Schreiner, P. R. *J. Am. Chem. Soc.* **1998**, *120*, 4184. (f) Nicolaides, A.; Borden, W. T. *J. Am. Chem. Soc.* **1993**, *115*, 11951. (g) Wierschke, S. G.; Nash, J. J.; Squires, R. R. *J. Am. Chem. Soc.* **1993**, *115*, 11958. (h) Cramer, C. J.; Squires, R. R. *J. Phys. Chem. A* **1997**, *101*, 9191. (i) Cramer, C. J. *J. Am. Chem. Soc.* **1998**, *120*, 6261. (j) Gräfenstein, J.; Hjerpe, A. M.; Kraka, E.; Cremer, D. *J. Phys. Chem. A* **2000**, *104*, 1748.

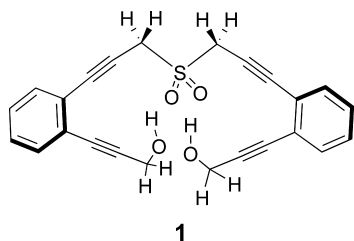


Figure 1. Optimized structure of the model system, bisenediynyl sulfone **1**.

comparatively rare.¹⁵ No computational study of GB cyclization has been reported to date. As both the MS and GB (for conjugated allene) cyclizations take place under ambient conditions, it is interesting as well as important to determine which process is more favored in a system equipped with structural features that permit both cyclization processes. Before embarking upon any experimental endeavor toward resolving the issue, we undertook a computational approach to see whether there is a definite preference for one over the other in a bisenediynyl sulfone system. This exercise pointed out a preference for GB over MS cyclization that was nicely proved by subsequent experiments.

Computational Study

We employed bisenediynyl sulfone **1** (Figure 1) as a model system in carrying out the theoretical calculation. We calculated the kinetic and thermodynamic parameters for both the MS and GB cyclizations for this system. It was expected that **1** under basic conditions would isomerize to form a system possessing the two moieties required for the MS and GB cyclizations, namely, an ene-yne-allene and a bisallenic sulfone, respectively.¹⁶

We first carried out a thorough conformational search for the ene-yne-allene system. Of the several conformational isomers, we chose only those two isomers that occupy minima in the potential energy surface and have the proper conformations for cyclization. These two isomers, **MS1** and **GB1**, are shown in Figure 2.

There is very little difference in energy ($\Delta E_{\text{GB1-MS1}} = 0.7$ kcal/mol) between these two isomers at the B3LYP/6-31G* level of theory. The conformation of isomer **GB1** is such that it can be considered as a bisallenic sulfone system, and hence, it is a potential candidate to undergo the GB reaction under suitable conditions. On the other hand, isomer **MS1** has a suitable conformation (ene-yne-allene) to undergo the MS reaction. In the present study, first we will discuss the complete mechanism of the GB reaction and then discuss the MS pathway.

The schematic representation of the GB pathway is shown in Scheme 3. The first step of the reaction is the formation of

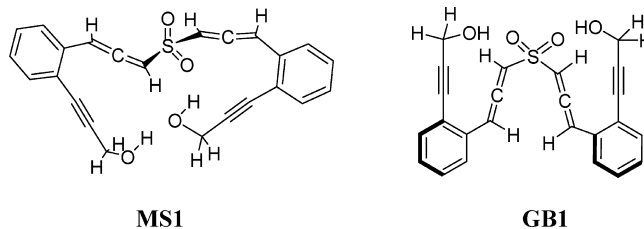


Figure 2. Optimized structures of the two isomers **MS1** and **GB1**.

a π/π benzylic biradical (**GB2**) as an intermediate. The energy barrier for the formation of biradical **GB2** from **GB1** is 24.4 kcal/mol at the B3LYP/6-31G* level of theory (Figure 3), and biradical **GB2** is 7.2 kcal/mol more stable than the reactant **GB1**. **GB2** undergoes two successive rotations, first along one of the C–C bonds (shown in red in Scheme 3) and then along another C–C bond (shown in green in Scheme 3), to form **GB4**. The energy barrier for the first rotation (along the C–C bond shown in red) is 6.4 kcal/mol. Biradical **GB3**, which is a rotamer of **GB2**, is almost equal in energy with **GB2**. The barrier for the second rotation (from **GB3** to **GB4**) is 9.0 kcal/mol. Cyclization of **GB4** leads to the formation of **GB5**. The structure **GB4** is 13.0 kcal/mol higher in energy than **GB5**, and the activation energy for this conversion (**GB4** to **GB5**) is 8.4 kcal/mol. Finally, **GB5** isomerizes to the product **GB6** via base-catalyzed tautomeric proton shifts.^{8e,13} A similar kind of highly exothermic H-atom shift accompanied by aromatization was extensively studied by Lewis and co-workers.¹⁷ The structure **GB6** is 63.2 kcal/mol more stable than **GB5**. The large thermodynamic stability of the product **GB6** is the main driving force for the reaction.

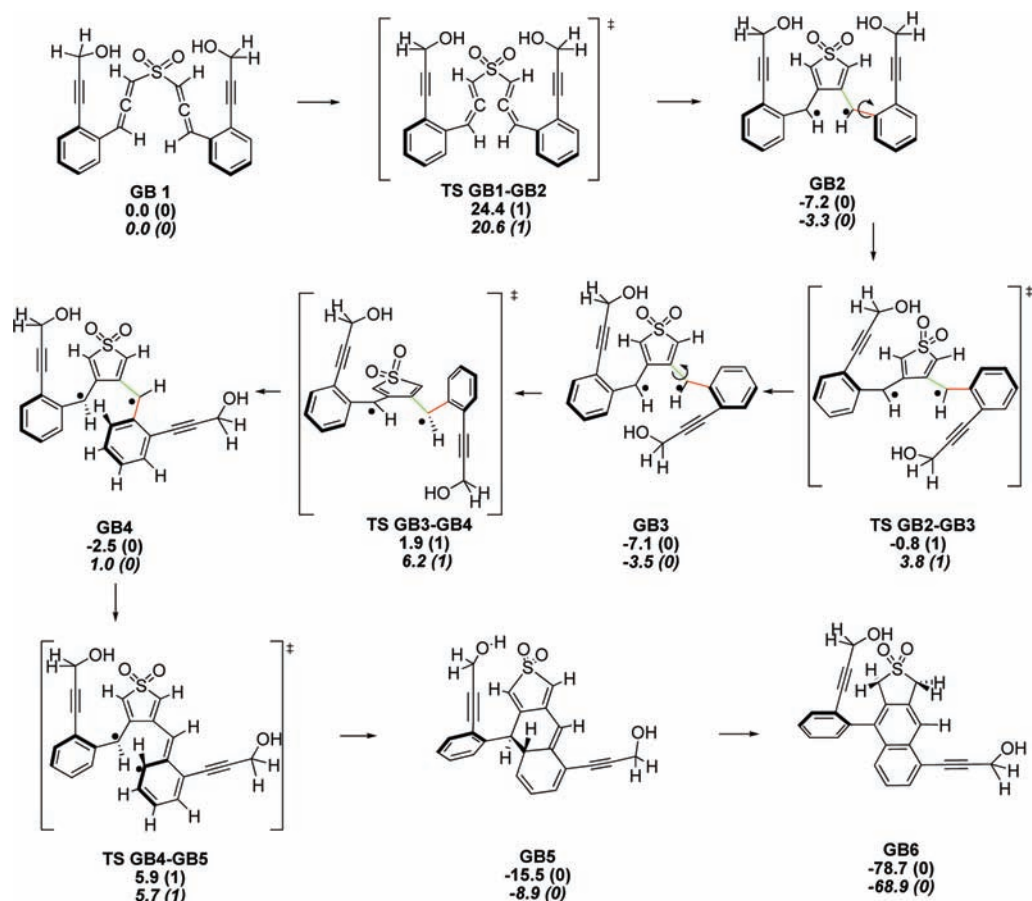
The schematic representation and the energetics of the MS pathway are shown in Scheme 4 and Figure 4, respectively. In this case also, the first step is the formation of a biradical, **MS2**, via a ring-closure mechanism. One of the key differences between the GB and MS mechanisms is the nature of the biradical species formed. In contrast to the GB reaction, the MS reaction produces a σ/π biradical intermediate. Biradical **MS2** is slightly more stable ($\Delta E_{\text{MS2-MS1}} = -0.3$ kcal/mol) than the reactant **MS1** at the B3LYP/6-31G* level of theory. The energy barrier for the conversion of **MS1** to **MS2** is 24.4 kcal/mol. Here, in order to compare the energetics of the different intermediates, which differ in the number of hydrogens, we have added suitable numbers of hydrogen molecules with the different intermediates. Unlike the GB pathway, where the biradical is self-quenched through intramolecular rearrangement processes, biradical **MS2** takes up two hydrogen atoms from the solvent to form **MS3**. In order to calculate the H-abstraction barrier in the MS pathway, we used 1,4-cyclohexadiene (1,4-CHD) as the H donor. The H-abstraction barrier at the σ radical position is 4.2 kcal/mol, whereas at the π radical position it is 10.2 kcal/mol (see the Supporting Information). A similar kind of ring closure takes place in the other part of the structure **MS3** to produce σ/π biradical **MS4** as an intermediate. The energy barrier for this cyclization is 27.0 kcal/mol. Finally, biradical **MS4** takes up two more hydrogen atoms from the solvent to produce the MS product **MS5**.

From the above mechanistic studies for the GB and MS processes, we found that the rate-determining step (rds) for the GB pathway is the formation of the π/π biradical **GB2** from

(15) (a) Schreiner, P. R.; Prall, M. *J. Am. Chem. Soc.* **1999**, *121*, 8615. (b) de Visser, S. P.; Filatov, M.; Shaik, S. *Phys. Chem. Chem. Phys.* **2001**, *3*, 1242.

(16) Although in principle the ene-yne-allene can also undergo Schmitt cyclization (SC) to form the fulvene diradical, we did not consider such a process in our theoretical calculations. Our chosen system is most likely to refrain from undergoing such a process, as Schmitt and co-workers have shown that only ene-yne-allenes with an aryl, silyl, or *tert*-butyl group attached to the alkyne terminus undergo SC. See: (a) Schmitt, M.; Strittmatter, M.; Mahajan, A. A.; Vavilala, C.; Cinar, M. E.; Maywald, M. *ARKIVOC* **2007**, *2007* (viii), 66. (b) Schmitt, M.; Strittmatter, M.; Stiffen, J.-P.; Maywald, M.; Engels, B.; Helten, H.; Musch, P. *J. Chem. Soc., Perkin Trans. 2* **2001**, 1331. (c) Schmitt, M.; Steffen, J.-P.; Angel, M. A. W.; Lennartz, C.; Hanrath, M. *Angew. Chem., Int. Ed.* **1998**, *37*, 1562. (d) Bekele, T.; Christian, C. F.; Lipton, M. A.; Singleton, D. A. *J. Am. Chem. Soc.* **2005**, *127*, 9216.

(17) Alabugin, I. V.; Manoharan, M.; Breiner, B.; Lewis, F. D. *J. Am. Chem. Soc.* **2003**, *125*, 9329.

Scheme 3. Garratt–Braverman Pathway for **GB1**^a

^a The relative energies and the number of imaginary frequencies (in parentheses) at B3LYP/6-31G* level of theory (values at BLYP/6-31G* level of theory are in italics) are given for different species involved in the reaction pathway.

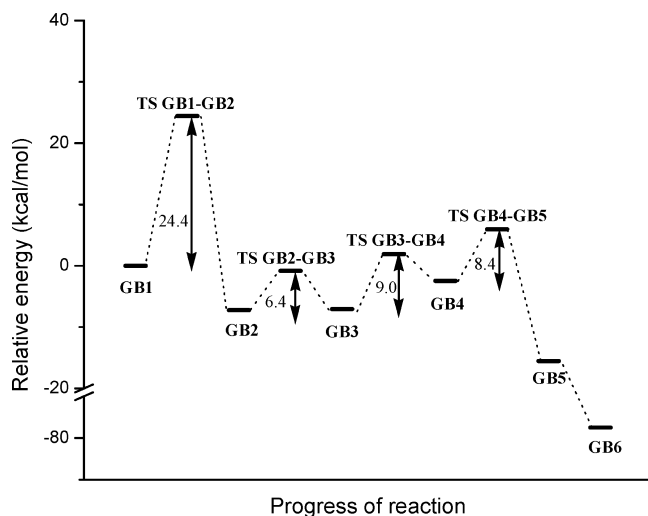


Figure 3. Reaction profile for the Garratt–Braverman mechanism.

GB1, whereas the rds for the MS pathway is the conversion of **MS1** to the σ/π biradical **MS2**. The activation energies for these two reactions are same (24.4 kcal/mol). Thus, from the kinetic point of view, both reactions are feasible. However, the main intermediate of the GB reaction (i.e., the π/π biradical **GB2**) is 6.2 kcal/mol lower in energy than the σ/π biradical **MS2** that is the main intermediate of MS reaction. This biradical formation step of the GB reaction is less endothermic than that of MS

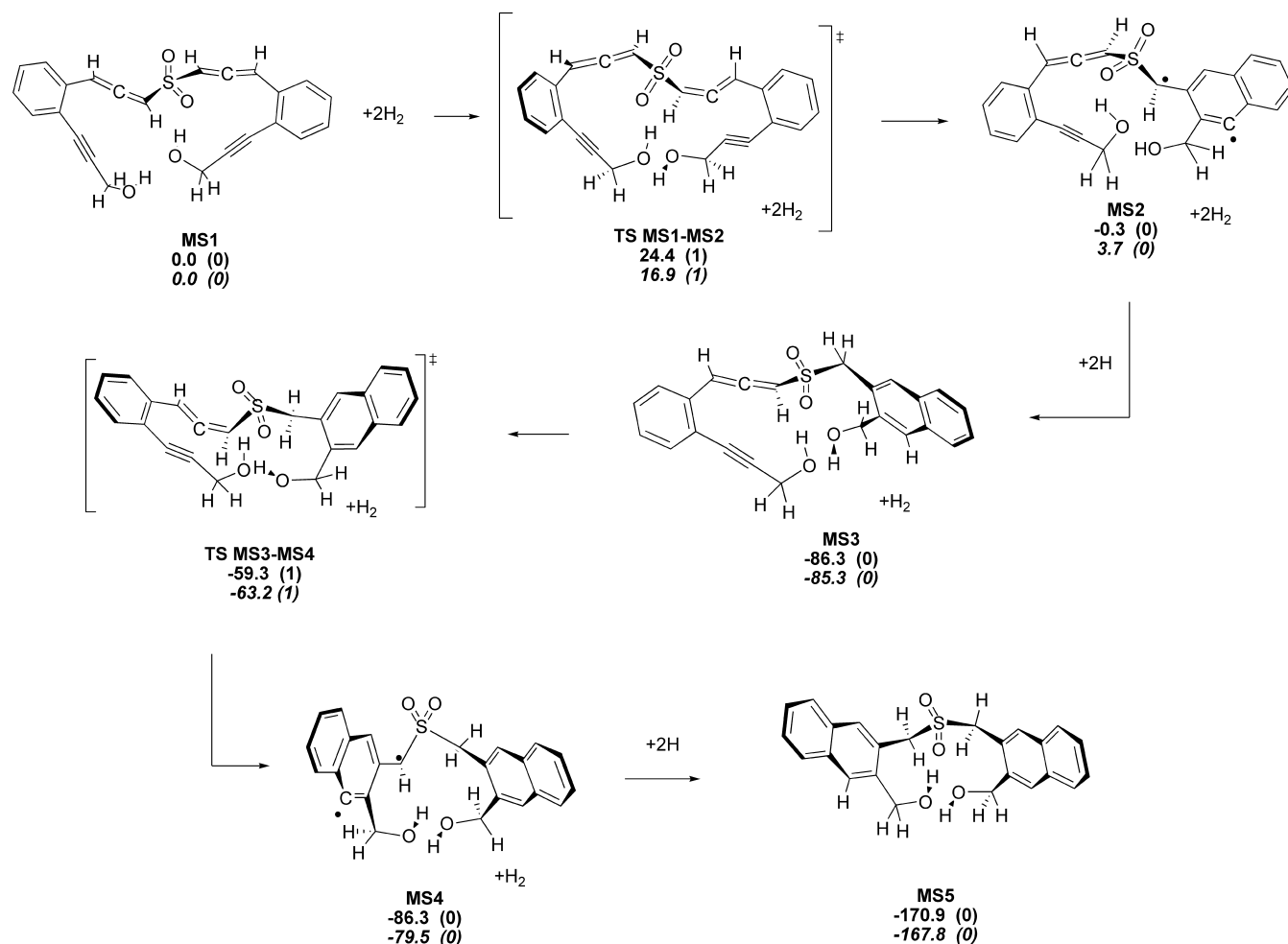
pathway, since a π radical on the benzylic methylene group is more stable than the σ radical of the **MS2** intermediate **MS2**. The higher stability of the π radical is partly due to conjugation with the aromatic ring and partly due to the fact that the alkyl–H bond is intrinsically weaker than the aryl–H bond.¹⁸ Thus, GB cyclization is thermodynamically favored over MS cyclization. If we compare the reverse of the reactions for the formation of the biradicals for the GB and MS processes, we find that the activation energy for the conversion of **GB2** to **GB1** is 31.6 kcal/mol whereas that for the conversion of **MS2** to **MS1** is 24.7 kcal/mol. Thus, biradical **GB2** is also kinetically more stable than biradical **MS2**. One may argue that the presence of the electron-withdrawing sulfonyl group disfavors the MS pathway. However, calculations done on a series of ene-yne-allenes with different electron-withdrawing substituents at the allene terminus showed that there is actually a decrease in the activation energy barrier for the biradical formation step (see the Supporting Information).

Computational Details

All of the computations were performed with the Gaussian 03 software package.¹⁹ All optimizations of ground-state geometries were done using the hybrid Hartree–Fock (HF)–density functional

(18) Koga, N.; Morokuma, K. *J. Am. Chem. Soc.* **1991**, *113*, 1907.

(19) Frisch, M. J.; et al. *Gaussian 03*, revision C.02; Gaussian, Inc.: Wallingford, CT, 2004.

Scheme 4. Myers–Saito Pathway for MS1^a

^a The relative energies and the number of imaginary frequencies (in parentheses) at B3LYP/6-31G* level of theory (values at BLYP/6-31G* level of theory are in italics) are given for different species involved in the reaction pathway.

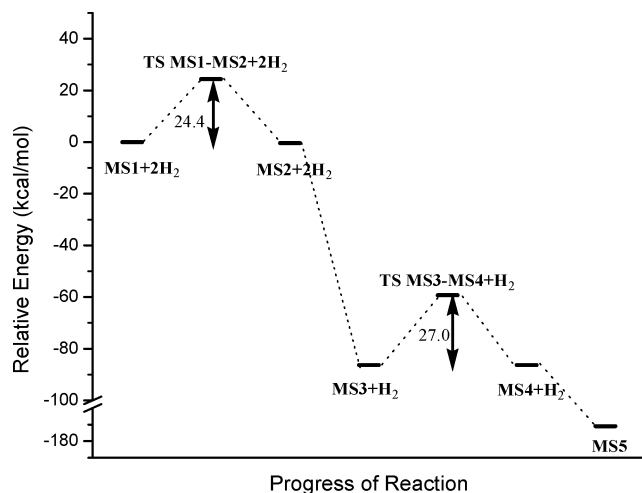


Figure 4. Reaction profile for the Myers–Saito mechanism.

theory (DFT) method B3LYP,^{20,21} based on Becke's three-parameter functional including the HF exchange contribution with a nonlocal correction for the exchange potential proposed by Becke together with the nonlocal correction for the correlation energy

(20) Hehre, W.; Radom, L.; Schleyer, P. v. R.; Pople, J. A. *Ab Initio Molecular Orbital Theory*; Wiley: New York, 1986.

suggested by Lee et al. The 6-31G* basis set was used for all of the calculations.¹⁹ A restricted approach was used in the computational analysis for the closed-shell structures, whereas an unrestricted broken-spin-symmetry approach (UBS-B3LYP) was used for the open-shell singlet-state transition states and intermediates. To get the broken-spin-symmetry solutions, we fed the SCF computation with a 50:50 mix (singlet–triplet) initial guess of the HOMO and LUMO orbitals. This approach worked acceptably well for the biradical intermediates and the transition states of the GB reaction, but for the MS biradicals, this approach was problematic, as the HOMO and LUMO for these biradicals do not correspond to the orbitals required for proper mixing. In these cases, we used permuted orbitals DFT (PO-DFT), as suggested by Cremer and co-workers,²² to calculate the open-shell singlet state. Schreiner et al.²³ had suggested that gradient-corrected generalized gradient approximation (GGA) functionals²⁴ such as BLYP are superior to hybrid functionals such as B3LYP for calculations on biradicals. We optimized all of the structures using the BLYP method with

- (21) (a) Becke, A. D. *J. Chem. Phys.* **1993**, *98*, 5648. (b) Becke, A. D. *Phys. Rev. A* **1988**, *38*, 3098. (c) Lee, C.; Yang, W.; Parr, R. G. *Phys. Rev. B* **1988**, *37*, 785. (d) Vosko, S. H.; Wilk, L.; Nusair, M. *Can J. Phys.* **1980**, *58*, 1200.
- (22) Gräfenstein, J.; Kraka, E.; Filatov, M.; Cremer, D. *Int. J. Mol. Sci.* **2002**, *3*, 360.
- (23) Schreiner, P. R.; Vazquez, A. N.; Prall, M. *Acc. Chem. Res.* **2005**, *38*, 29.
- (24) Koch, W.; Holthausen, M. C. *A Chemist's Guide to Density Functional Theory*; Wiley-VCH: Weinheim, Germany, 2000.

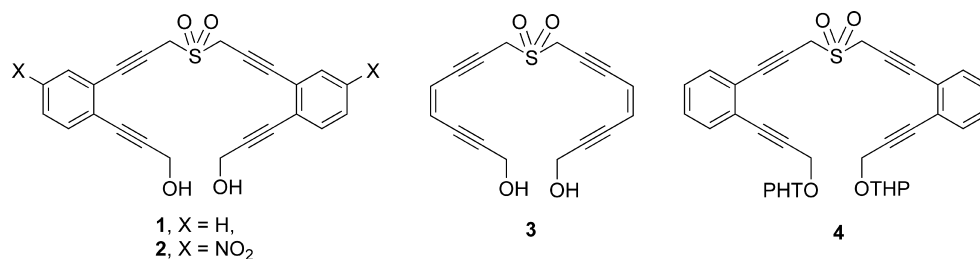
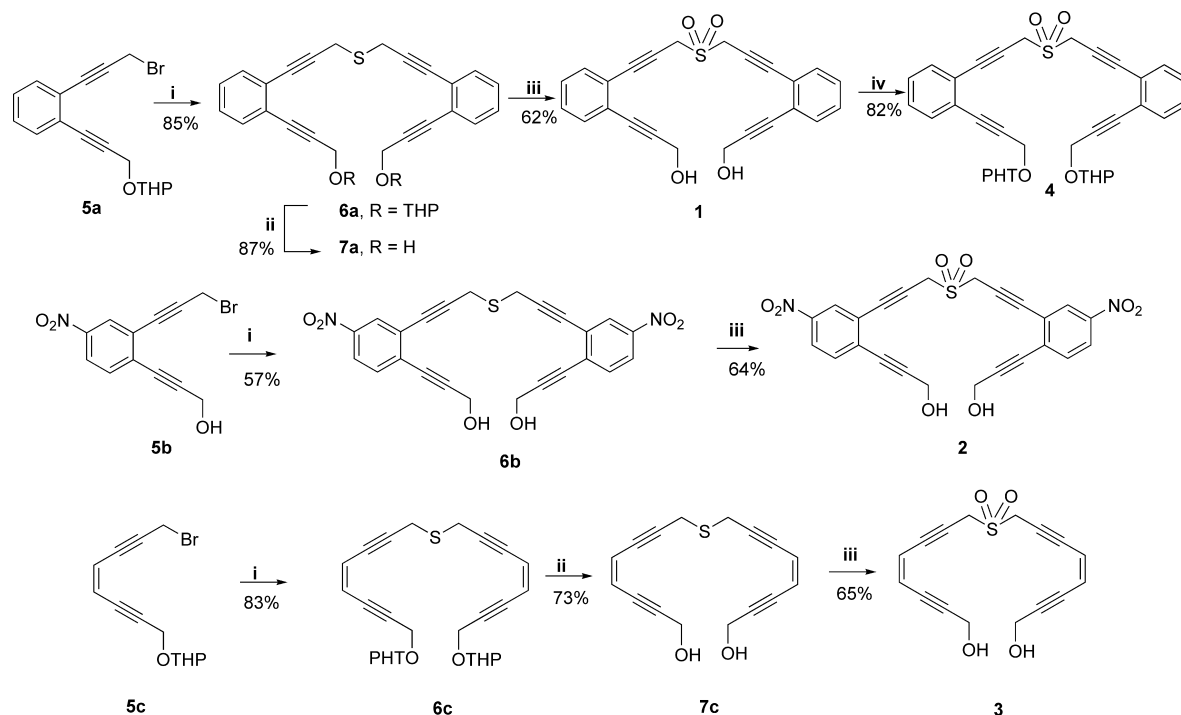


Figure 5. Target bispropargyl sulfones 1–4.

Scheme 5. Synthesis of Sulfones^a



^a (i) Na₂S, dry MeOH; (ii) PPTS (catalytic), EtOH; (iii) *m*-CPBA, dry CH₂Cl₂; (iv) DHP, PPTS (catalytic), dry CH₂Cl₂.

the same basis set, and the results were very much comparable with the earlier method. The nature of the stationary points was characterized by vibrational frequency calculations.

Experimental Work

With the computational exercise favoring GB over MS cyclization, we set out to prove the experimental validity of the theoretical prediction. For that task, we designed and subsequently synthesized bis(enediynes)sulfones 1–4 (Figure 5).

Sulfones 1–4 were synthesized in a straightforward manner, as shown in Scheme 5. The key step was the formation of the tetrahydropyran (THP)-protected thiobisenediynyl diol 6a by the reaction of bromide 5a with Na₂S in a 2:1 ratio in methanol. Deprotection followed by oxidation of sulfide 7a led to the formation of sulfone 1. The bis-THP-protected sulfone 4 was prepared via protection of diol 1. Direct oxidation of THP-protected sulfide 6a with *m*-chloroperoxybenzoic acid (*m*-CPBA) led to the formation of several products, possibly due to partial deprotection. Nitro-substituted sulfone 2 and nonbenzenoid sulfone 3 were prepared in a similar way from bromides 5b and 5c, respectively. All of the sulfones were characterized by NMR and mass spectral data.

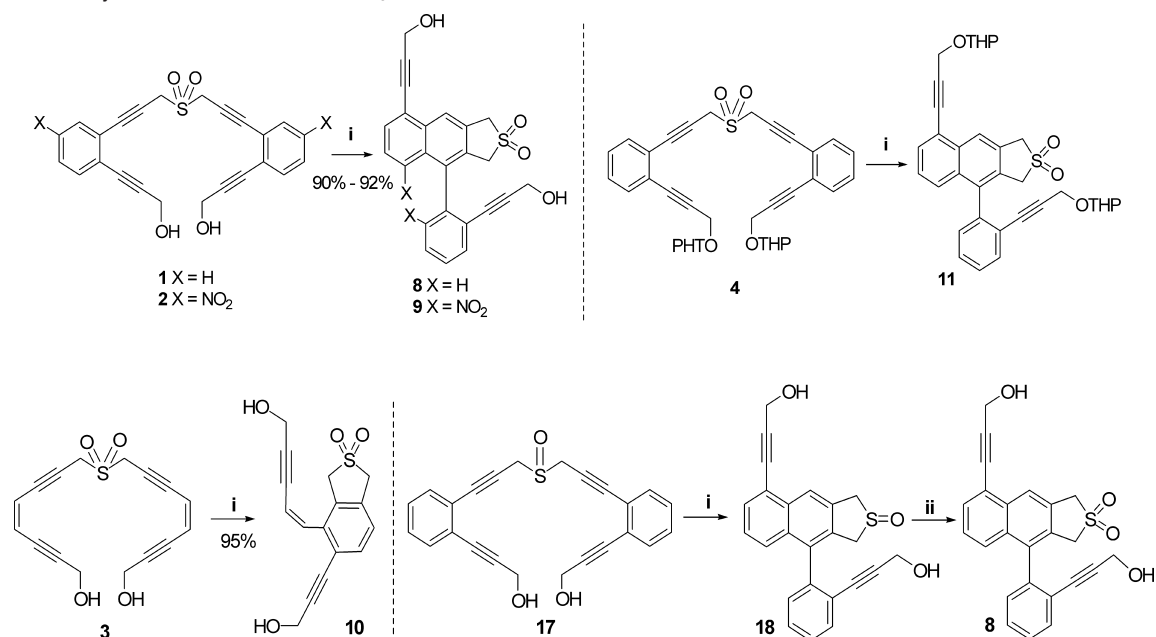
In an initial NMR experiment, sulfone 1 (10 mg) dissolved in CDCl₃ was treated with a catalytic amount of triethylamine,

and ¹H NMR spectra were recorded at different time points. The concentration of the starting material decreased with time while new peaks started to appear. The transformation was complete within 2 h. The reaction was repeated in benzene and triethylamine, and the same product, characterized as 8, was isolated in 90% yield (Scheme 6).

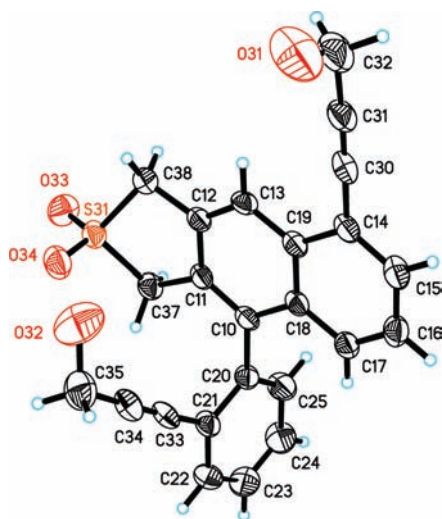
Structure elucidation was done on the basis of NMR and mass spectral data. For example, compound 8 showed the presence of four acetylenic carbons and new aromatic protons indicating the occurrence of cycloaromatization. The mass spectrum of 8 showed a molecular ion peak at *m/z* 403. Final confirmation of the structure was obtained from single-crystal X-ray analysis²⁵ (the ORTEP diagram is shown in Figure 6). Similar results were obtained for the nitro-substituted and aliphatic enediynes, which gave products 9 and 10, respectively, in quantitative yield (Scheme 6). Of these propargyl sulfones, the reaction with the nitro-substituted one was the fastest, with the conversion over within 30 min.

The mechanism of formation of the product is shown in Scheme 7. This is according to what has been proposed by

(25) The crystal structure has been deposited at the Cambridge Crystallographic Data Centre and has been allocated the deposition number CCDC 722767.

Scheme 6. Reactivity of Various Sulfoxes with Et₃N^a

^a (i) CDCl₃, Et₃N; (ii) *m*-CPBA, dry CH₂Cl₂.

Figure 6. X-ray structure of product **8**.

Braverman.^{8e,13} The initial bisallenenes **12** undergo GB cyclization to yield the dihydronaphthalene derivatives **14**, which isomerize to the product **8** via a base-catalyzed tautomeric shift (pathway **a**). The alternate MS cyclization (pathway **b**) was not followed at all. It may be argued that the outcome of the reaction might change in the presence of an external H donor. We repeated the experiment in presence of up to 50 equiv of 1,4-CHD, but the outcome remained the same. We could detect the formation of only the GB product in the ¹H NMR spectra (see the Supporting Information). Though the computational study indicated a preference for the GB pathway over the MS pathway, the exclusive preference for the GB pathway, as found experimentally, demands a more concrete explanation. It is true that the higher stability of biradical **GB2** over biradical **MS2** definitely favors the GB pathway, but this may not be the sole reason that can explain the complete preference for the GB pathway. To analyze this issue, we once again carefully looked at both mechanisms. After the formation of **GB2**, the GB

pathway involves an intramolecular radical addition in which the effective molarities of the reacting parts of the molecule are very high, but the subsequent steps in MS pathway are intermolecular hydrogen abstractions for which the actual molarities of the H donors can never approach the effective molarities of the components in the GB pathway. Thus, the intramolecular self-quenching nature of the GB pathway may also play an important role in the exclusive preference for this reaction even in the presence of a large excess of external H donor.

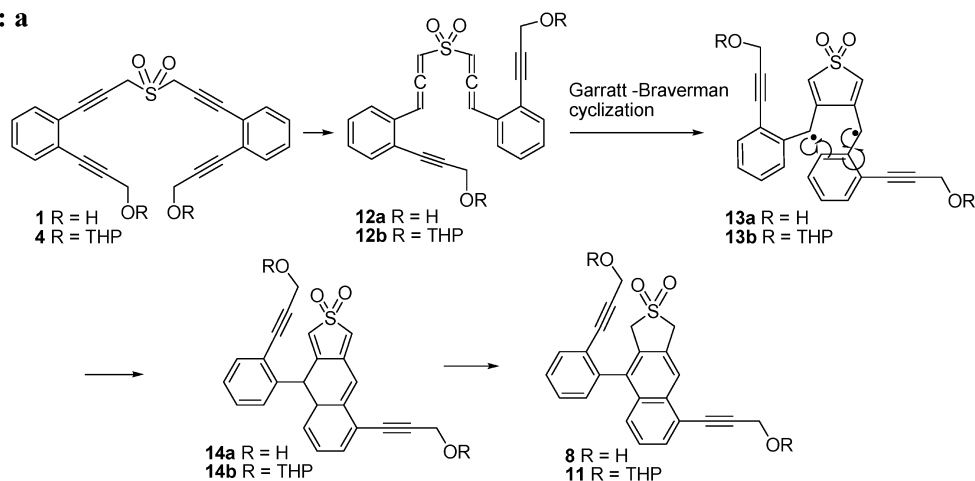
Having established that the GB cyclization is the sole path followed by these bisenediynyl sulfoxes, the reason for such a preference was then investigated from a chemical standpoint. First, we established the fact that there was no role of the hydroxyl groups in forcing the molecules to adopt a conformation suitable for GB cyclization by protecting the hydroxyl groups as THP ethers. Thus, bis-THP-protected sulfone **4** (actually a mixture of diastereomers), when subjected to triethylamine treatment, underwent GB cyclization to yield product **11** (Scheme 6). The ¹H NMR spectrum of the latter was very complicated because of the presence of various diastereomers. Hence, the THP groups were removed to produce a diol identical to **8** isolated earlier from reaction of **1**. Since bispropargyl sulfoxides are also reported to undergo GB cyclization upon base treatment,²⁶ we also prepared bisenediynyl sulfoxide **17** by carrying out the *m*-CPBA oxidation at 0 °C. The sulfoxide in CDCl₃, upon treatment with triethylamine (catalytic amount), again followed the same GB pathway (Scheme 6), although much more slowly (the time for completion was 24 h). In this case also, the structure was confirmed by oxidizing the product, **18**, to sulfone **1**.

A low-temperature ¹H NMR experiment was carried out to identify the intermediate (Figure 7). There was practically no reaction until the reaction temperature was raised to 15 °C. At that point, new peaks at δ ~4.4 and 4.3 started to appear. With time, these peaks started to disappear with concomitant appear-

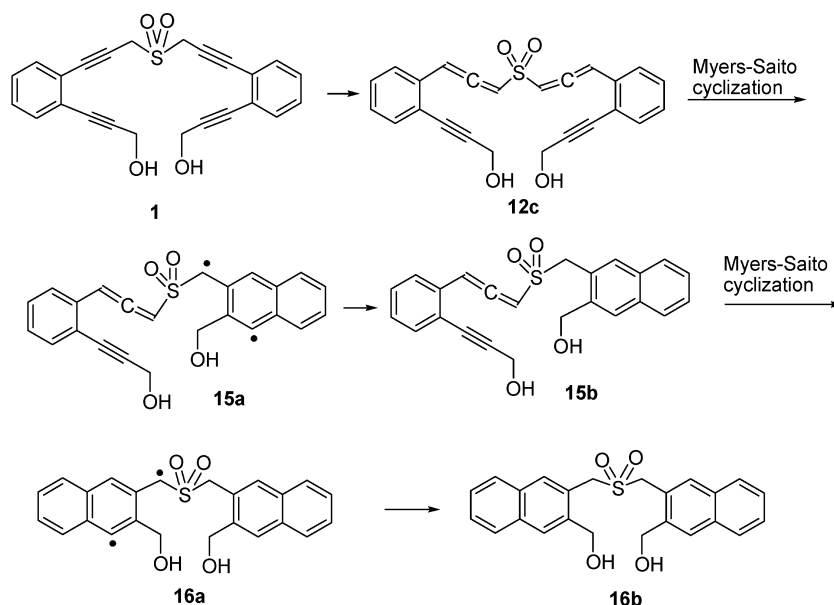
(26) Braverman, S.; Zafrani, Y.; Gottlieb, H. E. *Tetrahedron* **2001**, *57*, 9177.

Scheme 7. Mechanisms of Formation of Products

Pathway: a



Pathway: b



ance of the peaks corresponding to the product. This intermediate, we believe, is the cyclization product **GB5** that is rapidly converted to the final product via H shifts.

The end product of the GB biradical is a self-quenched diamagnetic species; hence, the possibility that the biradical will abstract an external hydrogen is slim. It is possible that biradicals that have an appreciable half-life will have enough time to abstract a hydrogen from an external source such as DNA and hence result in its damage. It may be mentioned that Braverman has reported²⁶ DNA cleavage by bispropargyl sulfones under basic conditions. We expected an inverse relation between the kinetics of cyclization of the sulfones and the kinetics of cleavage efficiency. Thus, sulfones **1–3** were incubated with pBR322 DNA at pH 8.5. Aliquots were taken at 10 and 60 min and subjected to agarose gel electrophoresis. The results are shown in Figure 8. It is evident that the benzene-fused bispropargyl sulfone has the highest cleavage efficiency, and the order followed is **1** > **3** > **2** (compound **2** seemed to have negligible activity). The faster collapse of the biradicals formed via GB cyclization lowered the prospect of DNA cleavage by H abstraction from the sugar moiety. The incubation results for THP-protected sulfone **4** and sulfoxide **17** showed higher

cleavage potential for the latter. In this case, the incubations were carried out for 24 h because of slow rearrangement. Thus, although the cleavage potentials are low, there is a fairly good correlation between the ease of rearrangement and the cleavage efficiency.²⁷

In conclusion, computational techniques were used to determine the preference between MS and GB cyclizations. The theoretical prediction that GB cyclization is favored over MS cyclization was nicely demonstrated by studying the reactivity of various bisenediynes sulfones. Currently we are exploring ways to change such a preference as well as the synthetic potential of the GB pathway.

Experimental Section

All of the ¹H and ¹³C NMR spectra were recorded at 400 and 100 MHz, respectively, in CDCl₃. The X-ray crystal data were recorded on Bruker AXS Smart Apex-II. Electrospray ionization (ESI) and high-resolution (HR) mass spectrometry (MS) were

(27) Sulfone **4** and sulfoxide **17** can inflict DNA cleavage even at a concentration of 50 μM (the gel picture is included in the Supporting Information).

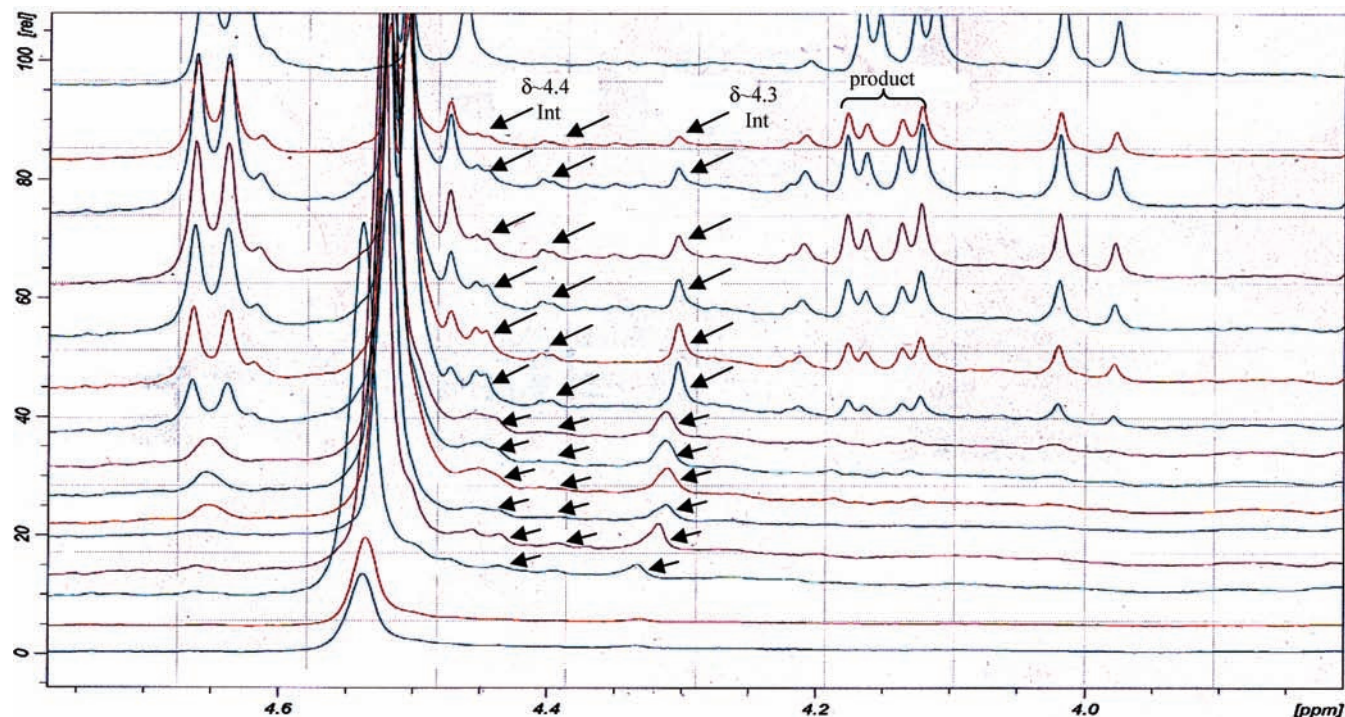


Figure 7. Low-temperature NMR spectra during the GB reaction of sulfone 1.

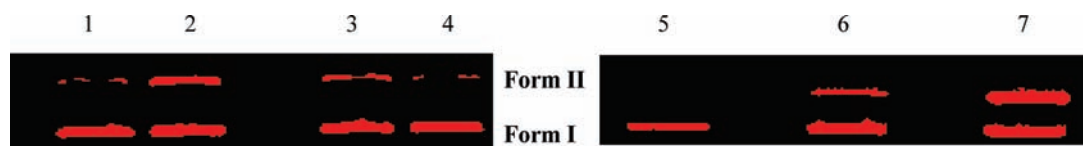


Figure 8. DNA cleavage studies with the sulfones. Lane 1: DNA (7 μL) in TAE buffer (pH 8.5) (5 μL) + DMSO (5 μL) at 23 $^{\circ}\text{C}$. Lane 2: DNA (7 μL) in TAE buffer (pH 8.5) (5 μL) + compound 1 in DMSO (1000 μM) at 23 $^{\circ}\text{C}$, 10 min. Lane 3: DNA (7 μL) in TAE buffer (pH 8.5) (5 μL) + compound 3 in DMSO (1000 μM) at 23 $^{\circ}\text{C}$, 10 min. Lane 4: DNA (7 μL) in TAE buffer (pH 8.5) (5 μL) + compound 2 in DMSO (1000 μM) at 23 $^{\circ}\text{C}$, 10 min. Lane 5: DNA (7 μL) in TAE buffer (pH 8.5) (5 μL) + DMSO (5 μL) at 23 $^{\circ}\text{C}$. Lane 6: DNA (7 μL) in TAE buffer (pH 8.5) (5 μL) + compound 4 in DMSO (1000 μM , 24 h) at 23 $^{\circ}\text{C}$. Lane 7: DNA (7 μL) in TAE buffer (pH 8.5) (5 μL) + compound 17 in DMSO (1000 μM , 24 h) at 23 $^{\circ}\text{C}$.

performed on a Waters LCT mass spectrometer; the solutions of the compounds were injected directly into the spectrometer via a Rheodyne injector equipped with 10 μL loop. A Phoenix 20 micro-LC syringe pump delivered the solution to the vaporization nozzle of the electrospray ion source at a flow rate of 10 $\mu\text{L min}^{-1}$. Nitrogen was used both as a drying gas and for nebulization with flow rates of $\sim 3 \text{ L min}^{-1}$ and 100 mL min^{-1} , respectively. The pressure in the analyzer region was usually $\sim 3 \times 10^{-5}$ torr.

Bis(3-(2-(3-(tetrahydro-2H-pyran-2-yloxy)prop-1-ynyl)phenyl)prop-2-ynyl)sulfane (6a). To a methanolic solution (5 mL) of bromide 5a (50 mg, 0.15 mmol), Na_2S (6 mg, 0.07 mmol) was added and the mixture was stirred for 30 mins at room temperature.²⁸ The mixture was evaporated to dryness and then worked up in the usual procedure. The title compound 6a was isolated by column chromatography (Si-gel, 7:1 PE/EA). State: yellow liquid. Yield: 85%. $^1\text{H NMR}$: δ 1.62–1.84 (12H, m) 3.5–3.53 (2H, m), 3.89–3.87 (6H, m), 4.54 (4H, ABq, $J = 8.8 \text{ Hz}$), 5.29 (2H, bs), 7.23–7.26 (4H, m), 7.41–7.46 (4H, m). $^{13}\text{C NMR}$: δ 19.0, 20.1, 25.3, 30.2, 54.8, 61.9, 81.9, 84.4, 88.9, 89.1, 96.6, 125.4, 125.6, 127.8, 128.0, 131.9, 132.2. EI-MS: m/z 539.4 (MH^+). HRMS: calcd for $\text{C}_{34}\text{H}_{34}\text{O}_4\text{S} + \text{H}^+$, 539.2258; found, 539.2262.

2,2'-(4Z,4'Z)-8,8'-Sulfonylbis(octa-4-en-2,6-diyne-8,1-diyl)bis(oxy)bis(tetrahydro-2H-pyran) (6c). Compound 6c was prepared from bromide 5c in essentially the same manner as described for 6a. State: pale-yellow liquid. Yield: 83%. $^1\text{H NMR}$: δ 1.54–1.86

(12H, m), 3.52–3.55 (2H, m), 3.69 (4H, s), 3.81–3.86 (2H, m), 4.46 (4H, ABq, $J = 16.0 \text{ Hz}$), 4.86 (2H, bs), 5.84 (4H, bs). $^{13}\text{C NMR}$: δ 19.0, 20.0, 25.3, 30.2, 54.7, 61.9, 80.7, 83.0, 92.5, 93.0, 96.7, 119.5, 119.6. EI-MS: m/z 439.2 (MH^+). HRMS: calcd for $\text{C}_{26}\text{H}_{30}\text{O}_4\text{S} + \text{H}^+$, 439.1944; found, 439.1947.

3,3'-(2,2'-(3,3'-Thiobis(prop-1-yne-3,1-diyl))bis(4-nitro-2,1-phenylene)diprop-2-yn-1-ol (6b). This was prepared as described for 6a using 5b (50 mg, 0.17 mmol) and Na_2S (7 mg, 0.08 mmol). The crude material was purified by column chromatography (Si-gel, 2:1 PE/EA). State: yellow solid. Yield: 57%. Mp: 163 $^{\circ}\text{C}$. $^1\text{H NMR}$: δ 3.86 (4H, s), 4.59 (4H, s), 7.55 (2H, d, $J = 8.8 \text{ Hz}$), 8.09 (2H, dd, $J = 2.8, 8.8 \text{ Hz}$), 8.26 (2H, d, $J = 2.0 \text{ Hz}$). $^{13}\text{C NMR}$: δ 20.4, 51.4, 80.5, 82.8, 91.2, 96.6, 122.8, 126.7, 131.4, 132.6, 133.0, 146.8. EI-MS: m/z 461 (MH^+). HRMS: calcd for $\text{C}_{24}\text{H}_{16}\text{N}_2\text{O}_6\text{S} + \text{H}^+$, 461.0808; found, 461.0810.

3,3'-(2,2'-(3,3'-Thiobis(prop-1-yne-3,1-diyl))bis(2,1-phenylene)-diprop-2-yn-1-ol (7a). State: yellow liquid. Yield: 87%. $^1\text{H NMR}$: δ 3.85 (4H, s), 4.55 (4H, s), 7.25 (4H, bs), 7.42 (4H, bs). $^{13}\text{C NMR}$: δ 20.2, 51.4, 82.2, 84.1, 88.6, 91.5, 125.2, 125.3, 128.1, 128.2, 131.9, 132.0. EI-MS: m/z 371.3 (MH^+). HRMS: calcd for $\text{C}_{24}\text{H}_{18}\text{O}_2\text{S} + \text{H}^+$, 371.1107; found, 371.1111.

(4Z,4'Z)-8,8'-Thiodiocta-4-en-2,6-diyne-1-ol (7c). State: pale-yellow liquid. Yield: 73%. $^1\text{H NMR}$: δ 3.73 (4H, s), 4.48 (4H, s), 5.87 (4H, s). $^{13}\text{C NMR}$: δ 20.0, 51.5, 81.0, 82.8, 92.4, 96.0, 119.6, 119.8. EI-MS: m/z 171.2 (MH^+). HRMS: calcd for $\text{C}_{16}\text{H}_{14}\text{O}_2\text{S} + \text{H}^+$, 271.0793; found, 271.0796.

General Procedure for the Synthesis of Sulfones. To a CH_2Cl_2 (10 mL) solution of sulfide (0.1 mmol) at 0 $^{\circ}\text{C}$, *m*-CPBA (2 equiv)

(28) Cao, X.; Yang, Y.; Wang, X. *J. Chem. Soc., Perkin Trans. 1* 2002, 2485.

was added and the solution was stirred for 2 h at room temperature.²⁹ The reaction mixture was then diluted with CH₂Cl₂ (20 mL), and the organic layer was washed successively with aqueous saturated NaHCO₃, saturated Na₂SO₃, and saturated Na₂CO₃ (30 mL each). The organic layer was evaporated to dryness, and the residue upon chromatography (Si-gel, 2:1 PE/EA) furnished the desired compound.

3,3'-(2,2'-(3,3'-Sulfonylbis(prop-1-yne-3,1-diyl))bis(2,1-phenylene))diprop-2-yn-1-ol (1). State: yellow viscous liquid. Yield: 62%. IR (neat) ν_{\max} (cm⁻¹): 9449, 2925, 2068, 1638, 1327, 1219, 1126, 1024, 769. ¹H NMR: δ 4.50 (4H, s), 4.51 (4H, s), 7.25–7.32 (4H, m), 7.43–7.44 (4H, m). ¹³C NMR: δ 44.5, 51.3, 79.3, 83.3, 86.9, 92.3, 123.8, 125.9, 128.1, 129.0, 131.8, 131.9. ESI-MS: m/z 403 (MH⁺). HRMS: calcd for C₂₄H₁₈O₄S + H⁺, 403.1005; found, 403.1009.

3,3'-(2,2'-(3,3'-Sulfonylbis(prop-1-yne-3,1-diyl))bis(4-nitro-2,1-phenylene))diprop-2-yn-1-ol (2). State: yellow solid. Yield: 64%. Mp: 212–216 °C. IR (KBr) ν_{\max} (cm⁻¹): 3426, 2365, 2345, 1637, 1517, 1346, 1220, 1028, 900, 873, 836, 772, 745. ¹H NMR: δ 4.51 (4H, s), 4.56 (4H, s), 7.57 (2H, d, J = 8.8 Hz), 8.15 (2H, dd, J = 2.0, 8.8 Hz), 8.29 (2H, d, J = 2.0 Hz). ¹³C NMR: δ 45.0, 51.3, 81.3, 82.0, 85.1, 97.9, 123.8, 125.0, 126.8, 132.1, 132.6. ESI-MS: m/z 493.06 (MH⁺). HRMS: calcd for C₂₄H₁₆N₂O₈S + H⁺, 493.0706; found, 493.0710.

(4Z,4'Z)-8,8'-Sulfonyldiocta-4-en-2,6-diyne-1-ol (3). State: pale-yellow liquid. Yield: 65%. IR (neat) ν_{\max} (cm⁻¹): 3441, 2365, 2345, 2066, 1637, 1126, 1016, 771. ¹H NMR: δ 4.37 (4H, d, J = 1.2 Hz), 4.48 (4H, d, J = 1.6 Hz), 5.92 (4H, ABq, J = 10.8 Hz). ¹³C NMR: δ 44.4, 51.3, 82.3, 82.8, 85.5, 96.5, 118.2, 122.2. ESI-MS: m/z 303.1 (MH⁺). HRMS: calcd for C₁₆H₁₄O₄S + H⁺, 303.0692; found, 303.0696.

2,2'-(3,3'-(2,2'-(3,3'-Sulfonylbis(prop-1-yne-3,1-diyl))bis(2,1-phenylene))bis(prop-2-yne-3,1-diyl))bis(oxy)bis(tetrahydro-2H-pyran) (4). A catalytic amount of pyridinium *p*-toluenesulfonate (PPTS) was added to a solution of sulfone **1** (22 mg, 0.05 mmol) in dry CH₂Cl₂ (5 mL). Dihydropyran (DHP) (11 μ L, 0.12 mmol) was then added dropwise, and the mixture was stirred at room temperature for 12 h.³⁰ Evaporation of the solvent in vacuum gave an oil from which title compound **4** was isolated by column chromatography (Si-gel, 4:1 PE/EA). State: yellow viscous liquid. Yield: 82%. IR (neat) ν_{\max} (cm⁻¹): 3450, 2946, 2369, 1653, 1637, 1338, 1128, 1077, 1024, 964, 942, 901, 813, 768. ¹H NMR: δ 1.53–1.83 (12H, m), 3.50–3.53 (2H, m), 3.8–3.86 (2H, m), 4.48–4.58 (8H, m), 4.87 (2H, t, J = 3.2 Hz), 7.25–7.32 (4H, m), 7.45 (4H, dd, J = 1.6, 7.2 Hz). ¹³C NMR: δ 19.0, 25.3, 30.2, 44.1, 54.7, 61.9, 80.1, 83.9, 86.2, 89.7, 96.8, 124.1, 125.8, 128.1, 128.8, 132.1, 132.4. ESI-MS: m/z 570.3 (MH⁺). HRMS: calcd for C₃₄H₃₄O₆S + H⁺, 571.2156; found, 571.2161.

3,3'-(2,2'-(3,3'-Sulfonylbis(prop-1-yne-3,1-diyl))bis(2,1-phenylene))diprop-2-yn-1-ol (17). To a solution of sulfide **1** (40 mg, 0.1 mmol) in CH₂Cl₂ (10 mL) at 0 °C was added *m*-CPBA (20 mg, 0.12 mmol), and the solution was stirred for 1 h at 0 °C.²⁸ The reaction mixture was then diluted with CH₂Cl₂ (20 mL), and the organic layer was washed successively with aqueous saturated NaHCO₃, Na₂SO₃, and Na₂CO₃ (30 mL each). The organic layer

was evaporated to dryness, and the residue upon chromatography (Si-gel, 1:2 PE/EA) furnished the desired compound. State: yellow solid. Mp: 260–262 °C (decomposition temperature). Yield: 87%. IR (neat) ν_{\max} (cm⁻¹): 3376, 2944, 2246, 1481, 1444, 1223, 1043, 1028, 952, 912, 759. ¹H NMR: δ 4.22 (4H, ABq, J = 16.4 Hz), 4.51 (4H, s), 7.23–7.3 (4H, m), 7.41–7.44 (4H, m). ¹³C NMR: δ 42.0, 52.2, 80.9, 83.6, 87.1, 92.6, 124.4, 125.8, 128.0, 128.7, 131.7, 131.8. ESI-MS: m/z 387.2 (MH⁺). HRMS: calcd for C₂₄H₁₈O₃S + H⁺, 387.1056; found, 387.1060.

General Procedure for Garratt–Braverman Reaction. Sulfone (10 mg) was taken in an NMR tube and dissolved in CDCl₃ (600 μ L). A catalytic amount of Et₃N (20 mol %) was added, and reaction was monitored by recording ¹H NMR spectra at different times. The reaction mixture was worked up using chloroform/water, and the final product was isolated by column filtration (Si-gel, 1:1 PE/EA).

Naphthosulfolene 8. State: yellow solid. Yield: 90%. Mp: 236–240 °C (decomposition temperature). IR (KBr) ν_{\max} (cm⁻¹): 3450, 2367, 2345, 2079, 1638, 1310, 1220, 1132, 1016, 770. ¹H NMR: δ 4.07, 4.32 (2 \times 2H, ABq, J = 16.4 Hz), 4.63, 4.67 (2 \times 2H, s), 7.26–7.27 (1H, m), 7.36–7.42 (2H, m), 7.47–7.48 (2H, m), 7.63–7.66 (1H, m), 7.71 (1H, d, J = 6.8 Hz), 8.38 (1H, s). ¹³C NMR: δ 51.0, 51.8, 55.7, 56.8, 82.6, 83.2, 92.2, 92.8, 120.4, 122.4, 123.8, 126.3, 126.8, 128.6, 128.7, 129.1, 129.2, 130.2, 131.5, 131.8, 132.9, 133.1, 136.6, 139.3. ESI-MS: m/z 403 (MH⁺), 425 (MNa⁺). HRMS: calcd for C₂₄H₁₈O₄S + H⁺, 403.1005; found, 403.1008.

Nitronaphthosulfolene 9. State: light-yellow solid. Yield: 92%. Mp: 310–322 °C (decomposition temperature). IR (KBr) ν_{\max} (cm⁻¹): 3436, 2918, 2850, 2345, 2367, 2067, 1637, 1342, 1028. ¹H NMR: δ 4.24, 4.30 (2 \times 2H, ABq, J = 16.0, 16.8 Hz), 4.68, 4.71 (2 \times 2H, s), 7.68 (1H, d, J = 7.6 Hz), 7.78 (2H, d, J = 8.8 Hz), 7.9 (1H, d, J = 2.0 Hz), 8.3 (1H, dd, J = 2.0, 8.4 Hz), 8.61 (1H, s). ¹³C NMR: δ 51.0, 51.6, 55.6, 56.4, 81.5, 81.6, 96.9, 98.1, 123.7, 124.1, 124.2, 125.3, 125.6, 129.1, 130.3, 131.4, 131.5, 133.6, 134.0, 134.4, 139.1, 146.4, 147.7. ESI-MS: m/z 493 (MH⁺). HRMS: calcd for C₂₄H₁₆N₂O₈S + Na⁺, 515.0525; found, 515.0533.

Benzosulfolene 10. State: white solid. Yield: 95%. Mp: 96–102 °C. IR (KBr) ν_{\max} (cm⁻¹): 3408, 2923, 2851, 2370, 1607, 1308, 1218, 1133, 1013, 772. ¹H NMR: δ 4.29, 4.39 (2 \times 2H, s), 4.51, 4.55 (2 \times 2H, s), 5.94 (1H, d, J = 11.6 Hz), 6.93 (1H, d, J = 11.6 Hz), 7.23 (1H, d, J = 8.0 Hz), 7.48 (1H, d, J = 8.0 Hz). ¹³C NMR: δ 51.3, 51.6, 56.1, 56.8, 82.1, 83.1, 93.6, 96.2, 113.4, 122.7, 125.2, 130.6, 131.8, 132.6, 136.6, 137.0. ESI-MS: m/z 303 (MH⁺). HRMS: calcd for C₁₆H₁₄O₄S + Na⁺, 325.0511; found, 325.0483.

Acknowledgment. D.M. and E.D.J. thank the SERC, IISc, for computational resources. DST is acknowledged for the J. C. Bose Fellowship Grant to E.D.J. and for a SERC Grant to A.B. that supported this research. S.D. is grateful to the CSIR, Government of India, for a senior research fellowship. The NMR and X-ray facilities were provided at IIT Kharagpur by DST under the IRPHA and FIST Programmes, respectively.

Supporting Information Available: Total energies, optimized Cartesian coordinates, various ¹H, ¹³C, and ¹H NMR kinetics spectra, a DNA-gel picture, complete ref 19, and crystallographic data for **8** (CIF). This material is available free of charge via the Internet at <http://pubs.acs.org>.

JA9023644

(29) (a) Nicolaou, K. C.; Zuccarello, G.; Riemer, C.; Estevez, V. A.; Dai, W. M. *J. Am. Chem. Soc.* **1992**, *114*, 7360. (b) Kar, M.; Basak, A. *Chem. Commun.* **2006**, 3818.

(30) Miyashita, M.; Yoshikoshi, A.; Grieco, A. P. *J. Org. Chem.* **1977**, *42*, 3772.